Integrative Biology

RSC Publishing

PAPER

View Article Online
View Journal

Cite this: DOI: 10.1039/c3ib20254b

Microdevice array-based identification of distinct mechanobiological response profiles in layer-specific valve interstitial cells†

Christopher Moraes,‡[ab] Morakot Likhitpanichkul,‡[a] Cameron J. Lam,[a] Bogdan M. Beca,[a] Yu Sun*[ab] and Craig A. Simmons*[ab]

Received 19th October 2012,
Accepted 26th January 2013

DOI: 10.1039/c3ib20254b

www.rsc.org/ibiology

Aortic valve homeostasis is mediated by valvular interstitial cells (VICs) found in spatially distinct and mechanically dynamic layers of the valve leaflet. Disease progression is associated with the pathological differentiation of VICs to myofibroblasts, but the mechanobiological response profiles of cells specific to different layers in the leaflet remains undefined. Conventional mechanically dynamic macroscale culture technologies require a large number of cells per set of environmental conditions. However, large scale expansion of primary VICs *in vitro* does not maintain *in vivo* phenotypes, and hence conventional macroscale techniques are not well-suited to systematically probe response of these cell types to combinatorially manipulated mechanobiological cues. To address this issue, we developed a microfabricated composite material screening array to determine the combined effects of dynamic substrate stretch, soluble cues and matrix proteins on small populations of primary cells. We applied this system to study VICs isolated from distinct layers of the valve leaflet and determined that (1) mechanical stability and cellular adhesion to the engineered composite materials were significantly improved as compared to conventional stretching technologies; (2) VICs demonstrate layer-specific mechanobiological profiles; and (3) mechanical stimulation, matrix proteins and soluble cues produce integrated and distinct responses in layer-specific VIC populations. Strikingly, myofibroblast differentiation was most significantly influenced by cell origin, despite the presence of potent mechanobiological cues such as applied strain and TGF-β1. These results demonstrate that spatially-distinct VIC subpopulations respond differentially to microenvironmental cues, with implications for valve tissue engineering and pathobiology. The developed platform enables rapid identification of biological phenomena arising from systematically manipulating the cellular microenvironment, and may be of utility in screening mechanosensitive cell cultures with applications in drug screening, tissue engineering and fundamental cell biology.

Insight, innovation, integration

Dynamic mechanical forces are critical features of the cardiovascular microenvironment, but are challenging to apply *in vitro*, particularly for high throughput screening purposes. In this work, we develop a composite material microfabricated culture platform to rapidly, systematically and combinatorially probe cellular response to applied deformation, soluble cues, and matrix proteins. We applied this technology towards identifying characteristic mechanobiological response profiles of valvular interstitial cells (VICs) isolated from distinct layers of the heart valve leaflet, and determined that these cells exhibit layer-specific sensitivity to combinations of mechanical, matrix and soluble factors. These findings demonstrate the importance of separately considering layer-specific VIC populations in tissue engineering and valve pathobiology studies, and demonstrate the necessity of using high-throughput approaches to probe these systems.

Introduction

Cyclic mechanical forces are critical features of the cardiovascular microenvironment, and play a pivotal role in regulating cell function, in combination with other environmental cues, such as matrix ligands and soluble signals.[1] Cells exhibit integrated phenotypic responses to combinations of microenvironmental parameters based on developmental, genetic

[a] Department of Mechanical and Industrial Engineering, University of Toronto, 5 King's College Road, Toronto, Ontario M5S 3G8, Canada. E-mail: simmons@mie.utoronto.ca, sun@mie.utoronto.ca; Fax: +1 416-978-7753; Tel: +1 416-946-0548, +1 416-946-0549

[b] Institute of Biomaterials and Biomedical Engineering, University of Toronto, 164 College Street, Toronto, Ontario M5S 3G9, Canada

† Electronic supplementary information (ESI) available. See DOI: 10.1039/c3ib20254b

‡ Authors contributed equally.

and environmental aspects of their history. Therefore, profiling these phenotypic responses in various cell populations can be important in identifying characteristic behaviours of specific cell types under various conditions, and understanding disease progression in complex heterogeneous tissue structures.

Profiling mechanobiological responses of various cell phenotypes requires the ability to systematically screen multiple combinatorially manipulated mechanobiological conditions. Current commercially available systems to apply cyclic stretch to cells *in vitro* lack the requisite experimental throughput. Recent technological advances have started to address the throughput limitation,[2–4] but have not effectively made the transition from the prototype stage to being a broadly-accepted tool for biological research, likely due to issues with fabrication, operational complexity and robustness.[5–12] In this work, we present a simple, mechanically dynamic, arrayed cell culture platform that enables combinatorial manipulation of critical mechanobiological parameters. We used the platform to identify differential mechanobiological response profiles of cells isolated from distinct layers of the aortic heart valve leaflet.

Aortic valve sclerosis is a common disease affecting 20–30% of the population over the age of 65, and is associated with a 50% increased risk of other cardiovascular disorders.[13] The disease is characterized by fibrotic thickening, the formation of focal subendothelial lesions, leaflet stiffening, imperfect coaptation, and disturbed hemodynamic flow.[14] The changes in the valve tissue that result in dysfunction are primarily mediated by valvular interstitial cells (VICs), which are primarily fibroblastic.[15] *In vivo* differentiation of VICs to myofibroblasts is correlated with the formation of lesions, matrix disarray, and fibrosis,[16–19] implicating myofibroblasts as having key roles in disease progression, likely through their increased contractility[20] and ability to remodel the extracellular matrix environment.[21,22]

The influence of multiple microenvironmental conditions on the differentiation of VICs to the myofibroblast state is poorly understood. VICs exist in a complex environment, and myofibroblast differentiation is known to be influenced by matrix stiffness,[23,24] mechanical stimulation,[25] chemical factors[26–28] and matrix proteins,[27] which potentially act in combination to regulate cell function.[29,30] Furthermore, although the valve is only a few hundred microns thick, valve composition is highly structured and organized, consisting of three distinct layers: the fibrosa on the aortic side; the spongiosa; and the ventricularis on the ventricular side. We hypothesized that VICs isolated from these spatially distinct regions exhibit differing myofibroblast differentiation potential in response to microenvironmental stimuli. This hypothesis is supported by the observations that layers exhibit differing matrix compositions *in vivo*,[31] that layers experience distinct mechanical conditioning stimuli as the leaflet bends,[32,33] and that focal lesions preferentially form in the fibrosa, whereas the ventricularis is relatively disease protected.[18] Endothelial cells on either side of the valve leaflet are known to exhibit distinct phenotypes[34] and responses to shear stress,[35] but side-specific dependency in the mechanical regulation of myofibroblast differentiation potential of VICs remains undefined.

To identify functional differences between the responses of layer-specific VICs to their microenvironment, it is necessary to screen cellular responses to multiple, combinatorially manipulated, mechanobiological parameters. The critical limitation in using conventional macroscale culture technologies to obtain these mechanobiological response profiles is the number of primary cells required. Extensive expansion of VICs on tissue culture plastic induces the myofibroblast phenotype,[16] and selectively biases the heterogeneous *in vivo* population distribution.[36] Conventional techniques are also poorly suited to address the number of combinatorially manipulated conditions to be screened.

In this work, we develop a microfabricated *in vitro* culture system designed to apply cyclic substrate strains to VICs from the fibrosa and the ventricularis, in combination with systematically manipulated chemical cues and matrix proteins. Using this platform, we demonstrate that mechanically induced myofibroblast differentiation of side-specific VICs is differentially modulated by matrix and soluble cues. These results demonstrate the potential for increased-throughput screening platforms in characterizing mechanobiological profiles, rapidly identifying biological phenomena of interest, and generating rational hypotheses for more specific mechanistic research.

Methods

Unless otherwise stated, all chemicals and reagents for cell culture were purchased from Sigma–Aldrich (Oakville, ON, Canada); fluorescent dyes from Invitrogen (Burlington, ON, Canada); and all other equipment and materials from Fisher Scientific Canada (Ottawa, ON, Canada).

Device overview

The microfabricated device consists of an array of suspended circular films. VICs cultured on the films experience radial and circumferential strains when the films are distended by the application of pressure, *via* a network of underlying PDMS microchannels (Fig. 1A and B). Groups of films are segregated using PDMS gaskets, enabling 12 combinations of matrix proteins, chemical cues and cell types to be simultaneously probed (Fig. 1C) on a $3'' \times 2''$ microfabricated device. In order to improve long-term adhesion between cells and the substrate, polyurethane (PU) culture films were integrated into the PDMS microfabrication process, using a modified version of a previously described technique.[37] Polyurethane can covalently bind matrix proteins,[37,38] enabling long-term culture, and presumably improve cell adhesion under cyclic load. However, free-standing films of PU were observed to exhibit mechanical creep over early cyclic loading, and hence are not suitable for this application. To address this issue, diaphragms consisting of a thick (45–100 μm) film of PDMS were layered with a thin (<1 μm) film of PU, to create a composite material structure, maintaining the advantages of PDMS in microfabrication and in mechanical elasticity, while improving cellular adhesion

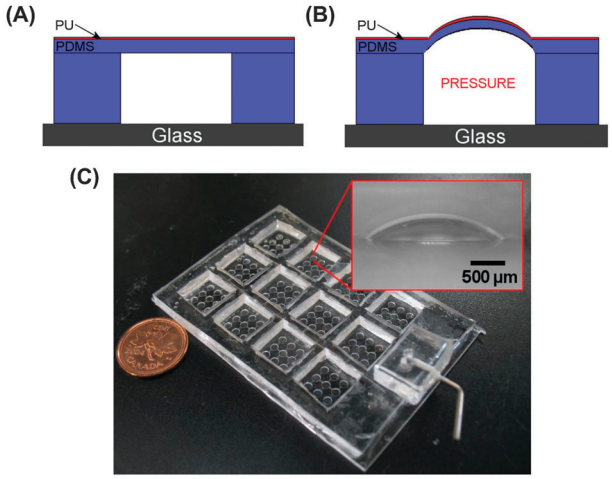

Fig. 1 Device overview. (A, B) Composite films consisting of a thick layer of PDMS and a thin layer of PU are (A) suspended over an actuation cavity; and (B) distended by the application of a pressure differential. (C) High-throughput system consisting of 12 segregated groups of 9 circular suspended films, fabricated on a 3″ × 2″ glass slide.

Table 1 Summary of device parameters and characterization results

Radius	Thickness	Pressure	Strain (within a 600 μm diameter ROI; mean ± upper/lower limit)	Nominal strain
1 mm	100 μm	6 kPa	Radial: 3.4 ± 0.3% Circumferential: 3.4 ± 0.3%	~3% (Low)
1 mm	45 μm	11 kPa	Radial: 12.4 ± 0.2% Circumferential: 11.3 ± 1.7%	~12% (High)

under cyclic mechanical load. Two types of devices with differing film thicknesses were selected to generate two distinct strain fields under differing pressures (parameters summarized in Table 1). Detailed fabrication and operation procedures for the microfabricated devices are provided in the online ESI† (Fig. S1).

System characterization

Characterization of surface strains was conducted by tracking the vertical displacement of fluorescent beads. Fluorescent polystyrene beads (Bangs Laboratories; Fishers, IN, USA) of 1 μm diameter were suspended in methanol and vortexed for 1 min to break up bead clusters. The solution was then pipetted onto the device surface and allowed to dry at ambient temperature. Confocal microscopy (Fluoview 300, Olympus Microscopes; Markham, ON, Canada) of the fluorescent beads was used to track diaphragm displacement at rest, and when actuated. Side-reconstruction of the confocal images (Fig. 2A and B) was used to determine vertical diaphragm displacement. An analytical model relating vertical deformation of clamped circular films to surface strains[39] was then used to determine the radial and circumferential surface strains generated (Fig. 2C; ESI†). This imaging and analysis procedure was repeated at intervals up to 10^5 actuation cycles to determine mechanical stability of the culture films under cyclic load.

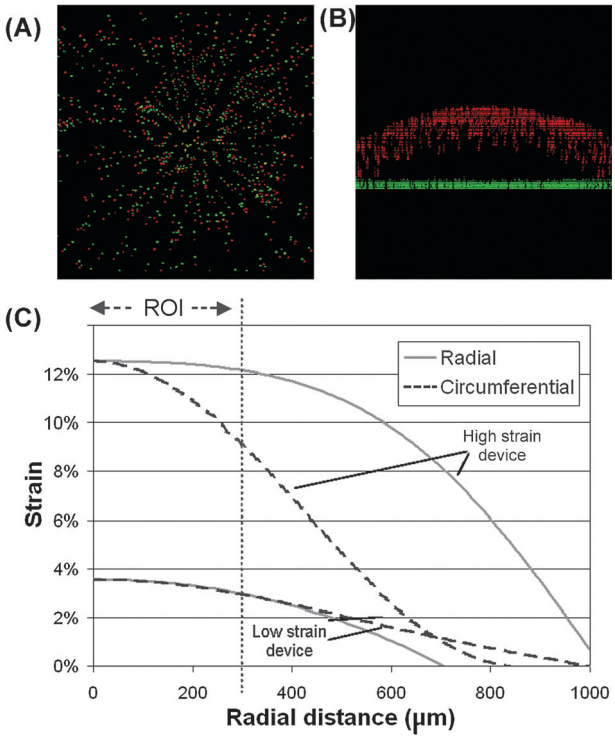

Fig. 2 Experimental strain characterization across device surface. (A, B) Fluorescent beads were used to track vertical displacement of the culture film (green = bead locations at rest; red = bed locations when actuated). (A) Top view of bead displacement; and (B) resliced confocal image (side view) were used in conjunction with an analytical model to calculate (C) radial and circumferential strains across the device surface under two applied pressure differentials (parameters summarized in Table 1). A selected region of interest (ROI) was used to minimize strain variations across the surface, while maintaining a sizeable culture area for VICs.

A sub-region of the device surface, a 600 μm diameter circle concentric with the circular film, was selected as the analysis region of interest (labeled 'ROI' in Fig. 2C), so as to minimize radial and circumferential strain variation across the device surface, while maintaining a large enough cell sample for analysis of myofibroblast differentiation. Each of the following analyses for cell experiments was limited to this region of the deforming substrate.

Device preparation and cell culture

Devices were sterilized, coated with saturating concentrations of covalently-bound Type I collagen or fibronectin, and pre-conditioned with supplemented DMEM for 2 hours at 37 °C prior to use. For adhesion studies, devices with and without the polyurethane layer were prepared and coated with collagen. Due to the scarcity of primary side-specific VICs, a mixed population of VICs (between passage two and five) was used to quantify adhesion differences arising from use of the composite films. Cells were seeded and allowed to spread on the device surface for 24 hours, and mechanically stimulated at ~12% cyclic strain at 1 Hz for an additional 24 hours. For the layer-specific studies, cells were isolated from the fibrosa and ventricularis layers of the valve leaflet (online ESI†). Less than 1%

of freshly isolated cells express SMA, as previously demonstrated by immunofluorescence of pooled[40] and side-specific cells.[24] Cells were grown in supplemented medium for no more than four population doublings (one passage) to more closely maintain an *in vivo* phenotype. Cell populations were then trypsinized using standard cell culture protocols, and seeded on the device surface at 15 000 cells per cm^2 in supplemented DMEM; with or without 5 ng mL^{-1} of transforming growth factor (TGF)-β1 (Chemicon; Temecula, CA, USA); and with or without 4 μM SD208, an inhibitor of the TGF-β receptor I-kinase. Cells were allowed to adhere and spread for 24 hours (37 °C, 5% CO_2) before the application of low (~3% strain) and high levels (~12% strain) of mechanical stimulation (at 1 Hz) for 24 hours. Cells were then fixed and stored at 4 °C for immunostaining and imaging.

Image analysis

Cell adhesion was assessed by counting the number of cells remaining on the nine mechanically active PDMS and PU-PDMS culture films in each well, and expressed as a percentage of the number of adherent cells on control (mechanically static) devices. After the stimulation period, cells were fixed and stained with a Hoechst 33258 nuclear dye. Results for cell counts on the mechanically active substrates are expressed as mean ± standard error percentages of the number of cells on the mechanically static samples (n = 6).

The incorporation of α-smooth muscle actin (SMA) into stress fibers is considered to be the defining characteristic of differentiated myofibroblasts,[22] and thus single cell immunofluorescence-based analysis is the most appropriate assay to identify the proportion of functional myofibroblasts in a heterogeneous population. To detect α-SMA expression, a standard immunocytochemistry procedure was followed, and myofibroblast differentiation was determined by counting the number of cells incorporating α-SMA into cytoskeletal stress fibers.[41] Results are expressed as mean ± standard deviations for each experimental condition (n = 7–8). All data was analyzed using multiple comparison ANOVA tests in SigmaStat 3.5 (Systat Software Inc.; San Jose, CA, USA). *Post-hoc* comparisons were conducted using the Tukey method.

Results

Characterization of mechanical strains

Measured deformation of the device surface enabled the calculation of strains applied to cells on the culture film. The radial and circumferential strains obtained for the two types of devices manufactured are shown in Fig. 2C. Limiting analysis area to a 600 μm diameter region of interest (ROI) was based on maximizing the number of cells available for analysis, while simultaneously providing distinctly different strain conditions in which the range of high strains is at least twice that of the range of low strains. Typical cell counts for this ROI ranged from 110 to 150 cells after 24 hours of cyclic stimulation at 1 Hz. The 600 μm diameter ROI produced a comparatively low strain field of 3.4 ± 0.3% in the radial and circumferential directions; and a comparatively high strain field of 12.4 ± 0.2% and 11.3 ± 1.7% in the radial and circumferential directions, respectively (Table 1). Nominal titular values of ~3% and ~12% are used for brevity in this discussion, and actual values are summarized in Table 1.

Composite film performance

Although free-standing PU films show greatly improved adhesion over PDMS,[37] the material undergoes creep, as evidenced by sagging in the culture films after cyclic actuation. Cyclic loading of the composite PU-PDMS films showed no discernible changes in strain over 100 000 actuation cycles (Fig. 3A), a result previously demonstrated for microfabricated PDMS films by us,[5] and for over 0.5 million cycles by other researchers.[42,43] Hence, inclusion of the PU coating does not appear to alter the mechanical stability of the PDMS films. Complete actuation

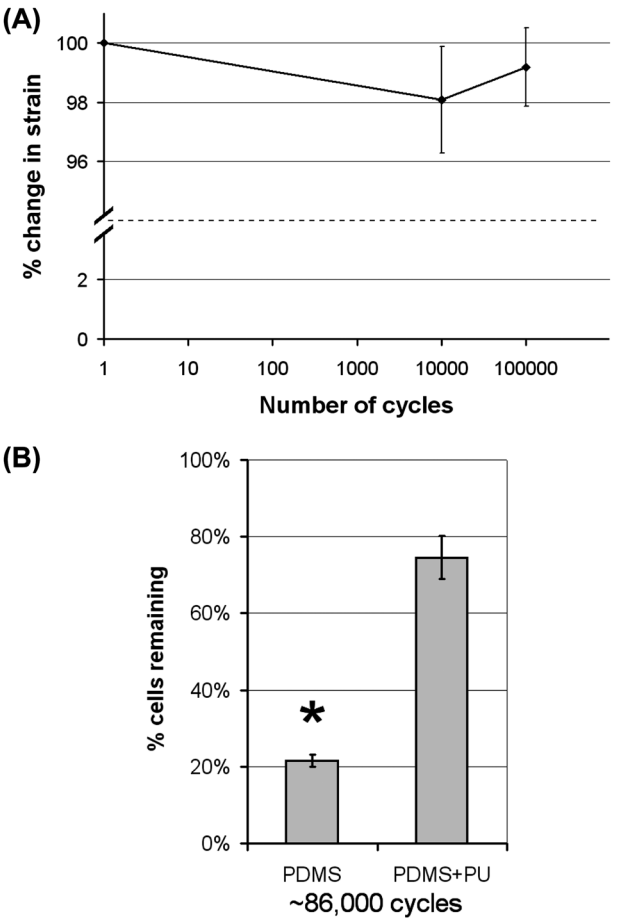

Fig. 3 Characterization of device operation over multiple actuation cycles. (A) Percent change in strain observed over 100 000 actuation cycles for a culture film undergoing ~12% strain, under cell culture conditions. In contrast to commercially available technologies, strain variation is minimal over the experimental period.[40] (B) Differences in VIC adhesion between collagen-coated PDMS-only devices and the collagen-coated PDMS + PU composite devices after 24 hours of mechanical stimulation (1 Hz) at ~12% strain. Results are normalized to static control samples (*$p < 0.001$), and demonstrate significant improvements in cell retention under cyclic dynamic mechanical load.

and relaxation of the bulging films were observed when using a square pressure waveform of 1 Hz frequency (Fig. S2, ESI†).

The use of the PU coating layer significantly improved adhesion over the actuated PDMS-only films, on which 20% of the primary cells remained adhered after 24 hours of cyclic stimulation at ~12% strain. In contrast, more than 75% of the cells cultured on the composite films remained adhered and well-spread under similar loading conditions (Fig. 3B).

Layer-dependent sensitivity of VICs to dynamic strain

No statistically significant loss of cells was observed in P1 side-specific VIC populations due to the applied mechanical strain ($p = 0.294$). The fraction of VICs expressing SMA stress fibers (as a marker of myofibroblasts) under each of the tested experimental conditions is reported in Fig. 4 (substrates coated with type I collagen) and Fig. 5 (substrates coated with fibronectin). In terms of individual culture parameters, cell origin (fibrosa *vs.* ventricularis) most strongly influenced myofibroblast differentiation across repeated experiments. Consistently increased levels of myofibroblast differentiation were observed in cells from the ventricularis over cells from the fibrosa for all culture conditions ($p < 0.001$). The presence of exogenous TGF-β1 also significantly increased myofibroblast differentiation in all conditions ($p < 0.05$).

Interaction effects between culture parameters were also significant. On collagen, increased differentiation of cells from the fibrosa occurred only at ~12% strain ($p < 0.001$), but the presence of TGF-β1 induced similar increases at both ~3 and ~12% strains, as compared to the static case ($p < 0.005$). Differentiation of ventricularis cells increased for both strain levels ($p < 0.001$), with or without TGF-β1. On the fibronectin-coated surfaces, differentiation of both cell populations was increased as compared to on collagen, but the effects of mechanical stimulation on the fibrosa cells were not statistically significant.

The dependence of fibronectin-induced myofibroblast differentiation of fibrosa VICs on the TGF-β1 pathway was tested by blocking the TGF-β1 Type II receptor with SD208. Use of the inhibitor did not result in a significant difference in

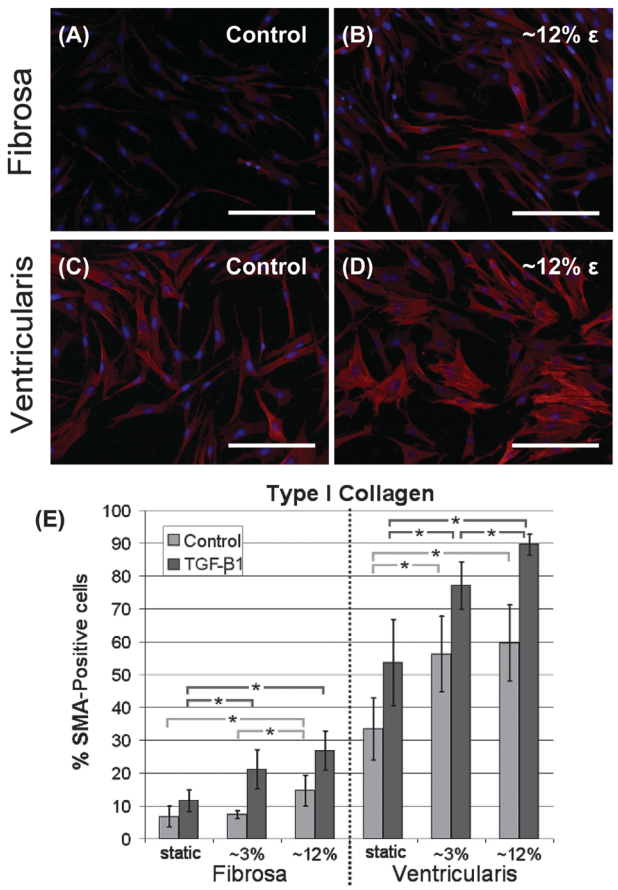

Fig. 4 Myofibroblast differentiation of side-specific VICs cultured on Type I collagen-coated surfaces. Representative images of cells from (A, B) the fibrosa; and (C, D) the ventricularis, cultured with 5 ng mL^{-1} TGF-β1 supplemented media under (A, C) no mechanical stimulation, and (B, D) ~12% cyclic strain. Scale bar = 100 μm. (E) Percentage of cells expressing the myofibroblast phenotype under combinatorially manipulated culture conditions, as characterized by localization of α-SMA in stress fibers. Selected statistical comparisons are highlighted (*$p < 0.01$, $n = 7$–8, experiment repeated three times).

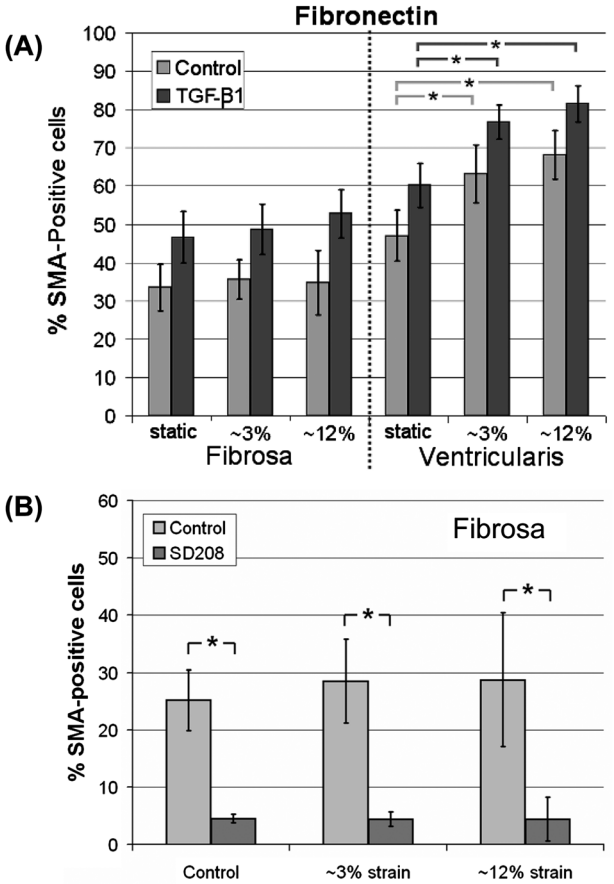

Fig. 5 Myofibroblast differentiation of side-specific VICs cultured on fibronectin-coated surfaces. (A) Percentage of cells expressing the myofibroblast phenotype under combinatorially manipulated culture conditions, as characterized by localization of α-SMA in stress fibers. Selected statistical comparisons are highlighted (*$p < 0.01$, $n = 7$–8, experiment repeated three times). (B) Effect of blocking the TGF-β Type II receptor on myofibroblast differentiation of fibrosa VICs cultured on fibronectin-coated substrates under varied mechanical stimulation (*$p < 0.001$, $n = 5$, experiment repeated twice).

cells remaining adhered to the substrate. Differentiation levels were reduced to a uniform baseline for all mechanical culture conditions ($p < 0.001$).

Discussion

Dynamic mechanical stimulation plays a critical role in regulating cellular function, in combination with other parameters in the cellular microenvironment. Dissecting cellular response to these combinations of parameters is challenging *in vivo,* and not possible with simple Petri dish *in vitro* culture systems. Furthermore, limited availability of primary cells precludes the use of macroscale culture equipment for combinatorially manipulated mechanobiological screening studies. This work presents a microfabricated system that bridges this gap, enabling increased-throughput fluorescent and morphological screening of mechanical, chemical and matrix cues on primary cells of limited availability. We utilized this system to study the mechanobiological myofibroblast differentiation response profile of cells from the fibrosa and ventricularis layers of the porcine aortic valve leaflet. Primary VICs cannot be expanded indefinitely, as extended culture of these cell types on tissue culture plastic has been shown to induce the myofibroblast phenotype[16] and alter the frequency of progenitor cells in this population.[36] Hence, given the limited number of cells that most closely reflect *in vivo* phenotypes, and the large number of environmental parameters that influence myofibroblast differentiation, a microfabricated platform for parallel testing is necessary.

The technology presented in this work addresses issues of device complexity, throughput, and cell adhesion, previously encountered by ourselves[5,8,44] and others.[6,7,9–11] This relatively simple device is easy to construct and is readily scaled up to mechanically stimulate greater numbers of cell populations. The development of the composite PU-PDMS films enables substantially improved adhesion of this cell type after 24 hours of cyclic stretch (Fig. 3B). Moreover, PU surface chemistry can be tailored for specific applications, and adhesion can be further strengthened using customized chemical modification and synthesis techniques developed by others,[45] potentially improving upon values reported here. Furthermore, polyurethane formulations can be customized and tailored for clinical applications, and polyurethane is commonly used as a scaffold material in tissue engineering.[46] Hence, use of this material could improve the clinical relevance of these studies and translational capacity of this technology. Alternatively, novel methods to bind stiffness-tunable polyacrylamide hydrogels to PDMS surfaces[47–49] are also compatible with this device, and in future may be used to modulate matrix stiffness in combination with applied cyclic strain.

Bolstering the poor fatigue resistance of PU with the thicker PDMS films enabled repeatable mechanical stimulation produced over 100 000 cycles. Measured strains were not significantly different during and after this loading regimen (Fig. 3A). This advantage in creating reproducible mechanical strains represents a significant improvement over current macroscale technologies, which have recently been shown to undergo cyclic strain-related fatigue as large as 21% of the nominal strain value, after as few as 10 000 cycles.[50] The resistance of thin PDMS films to mechanical fatigue has been demonstrated previously,[5] and may be a result of membrane thickness and uniformity obtained by microfabrication techniques. Although experiments reported in this work are limited to 24 hours of stimulation at 1 Hz, our experience and those of others[42,43] strongly suggests that longer experiments can be conducted.

The primary criticism of distending macroscale culture diaphragms by the application of a pressure differential is the non-uniformity of surface strains generated.[51] However, for techniques designed to provide an initial screen of cell function, careful characterization and selection of the analysis region of interest can mitigate these issues, although paracrine signaling between differentially stimulated populations remains a potential confounding factor. In this study, the analysis region was selected to maximize the number of cells studied, while generating mechanically distinct low ($\sim$3%) and high ($\sim$12%) strain fields across the ROI (Table 1; Fig. 2C). These values were chosen to bracket possible VIC deformation *in vivo,* based on work calculating a maximum of 11% tissue strain in the belly area of the valve leaflet,[52] from which the cells were isolated; and an understanding that transmitted strain can be attenuated between tissue and cell deformation.

The influences of matrix proteins, mechanical stimulation and chemical cues on myofibroblast differentiation have been generally established for fibroblasts.[21,22] The effects of TGF-β1,[27] and collagen and fibronectin matrix proteins[53] on myofibroblast differentiation specific to VICs have also been explored. The experimental platform developed in this work enables, for the first time, an examination of the relative influence of each of these parameters combinatorially on spatially segregated sub-populations of VICs, which have previously been considered to be the same cell population. While single-cell immunofluorescence assays are the most rigorous measure of myofibroblast differentiation for this particular study, this system could potentially be used in combination with novel isolation[54] and analytical techniques[55] to conduct assays applicable to a broader range of biological studies.

Interestingly, cell origin influenced pathological differentiation more strongly than microenvironmental conditions, including potent pathological cues such as applied deformation and the presence of TGF-β1. Combinatorial effects observed include the interactional effect between the presence of TGF-β1 and differing levels of mechanical stimulation: on the collagen-coated surfaces, fibrosa cells exhibit an increase in myofibroblast differentiation only at high strain levels, unless in the presence of TGF-β1, in which case increased levels are observed at low strains. This 'mechanical dose' dependency is also observed with cells from the ventricularis, in which higher strains increase differentiation (Fig. 4E).

The influence of matrix proteins on regulating response to mechanical stimuli appears to be critical in myofibroblast differentiation (Fig. 5A). Fibrosa VICs demonstrate increased myofibroblast differentiation on fibronectin coated substrates,

as compared to collagen-coated substrates. The effects of mechanical stimulation on fibronectin-stimulated cells from the fibrosa were not significant, while cells from the ventricularis continued to show significant responses to mechanical stimulation. This suggests that either (1) fibronectin alone ''saturates'' fibrosa cell myofibroblast differentiation, thereby 'washing out' any mechanical effects (though the significant increase in myofibroblast differentiation by the addition of TGF-β1 suggests that this is not the case), or (2) only a subset of the differentiated myofibroblasts are influenced by dynamic mechanical stimulation, or (3) that fibronectin inhibits the mechanical response of fibrosa VICs. Our previous work on collagen-coated substrates demonstrated that mechanical regulation of myofibroblast differentiation requires a permissive quantity of TGF-β1, usually sourced from the serum-supplemented medium in culture,[24] or produced endogenously by the VICs. Experiments in which the TGF-β receptor I-kinase was inhibited demonstrate that TGF-β1 remains a required component of this fibronectin-mediated, mechanically-independent myofibroblast differentiation mechanism (Fig. 5B).

Regardless of mechanism, these results demonstrate significant integrated matrix- and mechanically-dependent differences in behaviour from cells on either side of the valve leaflet, and further emphasize the need to screen mechanobiological response profiles in determining functional differences between cell populations. Speculatively, these differences in phenotypic responses may be due to environmental regulators, such as differing mechanical conditioning of the VICs in different layers,[32] or through spatially distinct endothelial cell-mediated signaling on the aortic and ventricular sides of the valve.[33,34] For example, cells in the fibrosa and ventricularis layers of the valve may have inherent or evolved mechanisms that protect the disease-prone cells from the distinct environmental stimuli on either side of the valve. Although further investigations into the reasons for these differences are required, taken together these data show distinct functional characteristics of cells from either side of the valve, and suggest distinct roles for the subpopulations in valve pathobiology and mechanobiology. More generally, as is the case with all cell culture models, these findings will also require further validation to ensure that the isolated cells mimic *in vivo* behaviour. Although well beyond the scope of this study, these challenging experiments may be conducted *ex vivo* using a bioreactor or *in vivo* using surgically altered animal models.

The microfabricated device developed for these studies allows for increased-throughput, long-term, combinatorial manipulation of mechanobiological culture parameters in the cellular microenvironment. Observing differential mechanobiological profiles in the limited number of cells available from separated layers of the valve leaflet in response to this variety of combinatorially manipulated parameters would require a substantial investment of time, reagents, and equipment using conventional approaches. This work demonstrates the potential for microdevices in screening for environmental parameters of interest when probing biological systems. As a result of scaling down the number of cells stimulated, these devices are best suited for fluorescent and morphological analyses, given the limited availability of biological material. Although the studies reported here demand single-cell fluorescent analyses, assay constraints for alternative applications may require the development of novel experimental techniques. However, in keeping with the growing commercial use of microscopy-based analyses for high-content and high-throughput screens, this platform is most broadly applicable in screening a broad range of microenvironmental conditions from which experimental focus can be narrowed and hypotheses generated for further investigation.

Disclosures

None

Acknowledgements

The authors would like to thank Christopher Yip and Gary Mo from the Center for Studies in Molecular Imaging for helpful discussions, microscopy expertise and use of equipment. We acknowledge microfabrication support from the Emerging Communications Technology Institute and the Toronto Microfluidics Foundry. We acknowledge financial support from the Natural Sciences and Engineering Research Council of Canada and the Canadian Institutes of Health Research (CHRPJ 323533-06), the Ontario Graduate Scholarship program to CM, and the Canada Research Chairs in Micro and Nano Engineering Systems to YS, and in Mechanobiology to CAS.

References

1 D. E. Ingber, *Ann. Med.*, 2003, **35**, 564–77.
2 D.-H. Kim, P. K. Wong, J. Park, A. Levchenko and Y. Sun, *Annu. Rev. Biomed. Eng.*, 2009, **11**, 203–233.
3 C. Moraes, Y. Sun and C. A. Simmons, *Integr. Biol.*, 2011, **3**, 959–971.
4 Kshitiz, J. Park, P. Kim, W. Helen, A. J. Engler, A. Levchenko and D.-H. Kim, *Integr. Biol.*, 2012, **4**, 1008–1018.
5 C. Moraes, J.-H. Chen, Y. Sun and C. A. Simmons, *Lab Chip*, 2010, **10**, 227.
6 W. Tan, D. Scott, D. Belchenko, H. J. Qi and L. Xiao, *Biomed. Microdevices*, 2008, **10**, 869–882.
7 Y. Kamotani, T. Bersano-Begey, N. Kato, Y.-C. Tung, D. Huh, J. W. Song and S. Takayama, *Biomaterials*, 2008, **29**, 2646–2655.
8 C. Moraes, R. Zhao, M. Likhitpanichkul, C. A. Simmons and Y. Sun, *J. Micromech. Microeng.*, 2011, **21**, 054014.
9 C. S. Simmons, J. Y. Sim, P. Baechtold, A. Gonzalez, C. Chung, N. Borghi and B. L. Pruitt, *J. Micromech. Microeng.*, 2011, **21**, 54016–54025.
10 K. Shimizu, A. Shunori, K. Morimoto, M. Hashida and S. Konishi, *Sens. Actuators, B*, 2011, **156**, 486–493.
11 T. K. Kim and O. C. Jeong, *Microelectron. Eng.*, 2012, **98**, 715–719.

12 C. Moraes, G. H. Wang, Y. Sun and C. A. Simmons, *Biomaterials*, 2010, **31**, 577–584.
13 C. M. Otto, B. K. Lind, D. W. Kitzman, B. J. Gersh and D. S. Siscovick, *New Engl. J. Med.*, 1999, **341**, 142–147.
14 B. A. Warren and J. L. Yong, *Pathology*, 1997, **29**, 360–368.
15 F. J. Schoen, *Cardiovasc. Pathol.*, 2005, **14**, 189–194.
16 M. Pho, W. Lee, D. R. Watt, C. Laschinger, C. A. Simmons and C. A. McCulloch, *Am. J. Physiol.*, 2008, **294**, H1767–H1778.
17 M. Olsson, M. Rosenqvist and J. Nilsson, *J. Am. Coll. Cardiol.*, 1994, **24**, 1664–1671.
18 C. M. Otto, J. Kuusisto, D. D. Reichenbach, A. M. Gown and K. D. O'Brien, *Circulation*, 1994, **90**, 844–853.
19 E. Rabkin, M. Aikawa, J. R. Stone, Y. Fukumoto, P. Libby and F. J. Schoen, *Circulation*, 2001, **104**, 2525–2532.
20 B. Hinz, G. Celetta, J. J. Tomasek, G. Gabbiani and C. Chaponnier, *Mol. Biol. Cell*, 2001, **12**, 2730–2741.
21 B. Hinz, *J. Biomech.*, 2010, **43**, 146–155.
22 J. J. Tomasek, G. Gabbiani, B. Hinz, C. Chaponnier and R. A. Brown, *Nat. Rev.*, 2002, **3**, 349–363.
23 C. Y. Y. Yip, J.-H. Chen, R. Zhao and C. A. Simmons, *Arterioscler., Thromb., Vasc. Biol.*, 2009, **29**, 936–942.
24 M. Likhitpanichkul, C. Y. Yip, W. L. K. Chen, K. Wyss, J.-H. Chen and C. A. Simmons, 2013, in submission.
25 J. Wang, H. Chen, A. Seth and C. A. McCulloch, *Am. J. Physiol.*, 2003, **285**, H1871–H1881.
26 G. A. Walker, K. S. Masters, D. N. Shah, K. S. Anseth and L. A. Leinwand, *Circ. Res.*, 2004, **95**, 253–260.
27 M. C. Cushing, J. T. Liao and K. S. Anseth, *Matrix Biol.*, 2005, **24**, 428–437.
28 M. C. Cushing, P. D. Mariner, J. T. Liao, E. A. Sims and K. S. Anseth, *FASEB J.*, 2008, **22**, 1769–1777.
29 J. H. Wang and B. P. Thampatty, *Biomech. Model. Mechanobiol.*, 2006, **5**, 1–16.
30 A. Grossi, K. Yadav and M. A. Lawson, *J. Biomech.*, 2007, **40**, 3354–3362.
31 N. Latif, P. Sarathchandra, P. M. Taylor, J. Antoniw and M. H. Yacoub, *J. Heart Valve Dis.*, 2005, **14**, 218–227.
32 J. De Hart, G. W. Peters, P. J. Schreurs and F. P. Baaijens, *J. Biomech.*, 2003, **36**, 103–112.
33 H. Y. Huang, J. Liao and M. S. Sacks, *J. Biomech. Eng.*, 2007, **129**, 880–889.
34 C. A. Simmons, G. R. Grant, E. Manduchi and P. F. Davies, *Circ. Res.*, 2005, **96**, 792–799.
35 P. Sucosky, K. Balachandran, A. Elhammali, H. Jo and A. P. Yoganathan, *Arterioscler., Thromb., Vasc. Biol.*, 2009, **29**, 254–260.
36 J. H. Chen, C. Y. Yip, E. D. Sone and C. A. Simmons, *The American journal of pathology*, 2009, **174**, 1109–1119.
37 C. Moraes, Y. K. Kagoma, B. M. Beca, R. L. M. Tonelli-Zasarsky, Y. Sun and C. A. Simmons, *Biomaterials*, 2009, **30**, 5241–5250.
38 Y. H. Li and Y. D. Huang, *J. Appl. Polym. Sci.*, 2006, **99**, 1832–1841.
39 E. Suhir, *Structural analysis in microelectronic and fiber-optic systems*, Van Nostrand Reinhold, New York, 1991.
40 K. Wyss, C. Y. Y. Yip, Z. Mirzaei, X. Jin, J.-H. Chen and C. A. Simmons, *J. Biomech.*, 2012, **45**, 882–887.
41 V. Dugina, L. Fontao, C. Chaponnier, J. Vasiliev and G. Gabbiani, *J. Cell Sci.*, 2001, **114**, 3285–3296.
42 J. Zhou and L. E. Niklason, *Integr. Biol.*, 2012, **4**, 1487–1497.
43 M. A. Unger, H.-P. Chou, T. Thorsen, A. Scherer and S. R. Quake, *Science*, 2000, **288**, 113–116.
44 M. T. Frey and Y. Wang, *Soft Matter*, 2009, **5**, 1918.
45 T. J. Dennes and J. Schwartz, *Soft Matter*, 2008, **4**, 86–89.
46 Q. P. Pham, U. Sharma and A. G. Mikos, *Tissue Eng.*, 2006, **12**, 1197–1211.
47 L. K. Fiddes, H. K. C. Chan, B. Lau, E. Kumacheva and A. R. Wheeler, *Biomaterials*, 2010, **31**, 315–320.
48 A. M. Throm Quinlan, L. N. Sierad, A. K. Capulli, L. E. Firstenberg and K. L. Billiar, *PLoS One*, 2011, **6**, e23272.
49 C. S. Simmons, A. Ribeiro and B. L. Pruitt, *Lab Chip*, 2013, **22**, 646–649.
50 F. H. Bieler, C. E. Ott, M. S. Thompson, R. Seidel, S. Ahrens, D. R. Epari, U. Wilkening, K. D. Schaser, S. Mundlos and G. N. Duda, *J. Biomech.*, 2009, **42**, 1692–1696.
51 T. D. Brown, *J. Biomech.*, 2000, **33**, 3–14.
52 J. Kortsmit, N. J. Driessen, M. C. Rutten and F. P. Baaijens, *Ann. Biomed. Eng.*, 2009, **37**, 532–541.
53 K. J. Rodriguez and K. S. Masters, *J. Biomed. Mater. Res.*, 2009, **90**, 1043–1053.
54 J. Kovac, Y. Gerardin and J. Voldman, *Adv. Healthcare Mater.*, 2012, DOI: 10.1002/adhm.201200196.
55 R. N. Zare and S. Kim, *Annu. Rev. Biomed. Eng.*, 2010, **12**, 187–201.

